



10 World Conference on Neutron Radiography 5-10 October 2014

Visualization of bulk magnetic properties by Neutron grating interferometry

B. Betz^{a,b,*}, P. Rauscher^c, R. Siebert^c, R. Schaefer^d, A. Kaestner^a, H. Van Swygenhoven^b,
E. Lehmann^a, C. Grünzweig^a

^aPaul Scherrer Institut, NIAG, Villigen-PSI, Switzerland

^bEcole polytechnique federale de Lausanne, NXMM laboratory, IMX, Lausanne, Switzerland

^cFraunhofer IWS Dresden, Ablation and cutting, Dresden, Germany

^dIFW Dresden, magnetic microstructures, Dresden, Germany

Abstract

The neutron Grating Interferometer (nGI) is a standard user instrument at the cold neutron imaging beamline ICON (Kaestner, 2011) at the neutron source SINQ at Paul Scherrer Institute (PSI), Switzerland. The setup is able to deliver simultaneously information about the attenuation, phase shift (DPC) (Pfeiffer, 2006) and scattering properties in the so-called dark-field image (DFI) (Grünzweig, 2008-I) of a sample. Since neutrons only interact with the nucleus they are often able to penetrate deeper into matter than X-rays, in particular heavier materials. A further advantage of neutrons compared to X-rays is the interaction of the neutron's magnetic moment with magnetic structures that allows for the bulk investigation of magnetic domain structures using the nGI technique (Grünzweig, 2008-II). The nGI-setup and its technique for imaging with cold neutrons is presented in this contribution. The main focus will be on magnetic investigations of electrical steel laminations using the nGI technique. Both, grain-oriented (GO) and non-oriented (NO) laminations will be presented. GO-laminations are widely used in industrial transformer applications, while NO-sheets are common in electrical machines. For grain-oriented sheet, domain walls were visualized individually, spatially resolved, while in NO-sheet a relative density distribution is depicted.

© 2015 The Authors. Published by Elsevier B.V. This is an open access article under the CC BY-NC-ND license (<http://creativecommons.org/licenses/by-nc-nd/4.0/>).

Selection and peer-review under responsibility of Paul Scherrer Institut

Keywords: Grating interferometry; magnetic structure; steel, scattering

* Corresponding author. Tel.: +41-56310-5829.

E-mail address: Benedikt.Betz@psi.ch

1. Introduction

1.1. Setup

The neutron grating interferometer consists of three gratings placed in the neutron beam, to observe the interference properties of the neutrons. There are the source grating G_0 (absorber grating) with a period of $1076 \mu\text{m}$, the beam splitter or phase grating G_1 with a period of $7.96 \mu\text{m}$ and the analyzer grating G_2 with $4 \mu\text{m}$ period (Grünzweig, 2008-III). A nGI setup is schematically shown in Figure 1. The source grating, placed close to the neutron beam exit port, allows for the use of an incoherent neutron source of a diameter c , typically $\sim 2 \text{ cm}$, since it transforms the source to an array of individual line sources of width $s \approx 600 \mu\text{m}$ (slit width). Each line provides enough spatial coherence for an interferometric contrast. The images created by each line superimpose congruently in the detector plane, leading to a gain in measured intensity. The moderate temporal coherence requirements of the nGI are satisfied by the use of a velocity selector providing, around the designed wavelength of $\lambda = 4.1 \text{ \AA}$, a bandwidth of: $\Delta\lambda/\lambda = 15 \%$. The phase G_1 grating is placed at a distance $l = 5.23 \text{ m}$ from G_0 and divides the incoming beam into its ± 1 diffraction orders (Grünzweig, 2007). The phase grating therefore acts as a phase mask for the neutrons and imprints periodic phase modulations onto the incoming waves. Through the Talbot effect (Talbot, 1836), the phase modulations are transformed into an intensity modulation in a plane, where G_2 is placed, at a distance of 19.4 mm , forming a linear periodic fringe pattern perpendicular to the optical axis and parallel to the grating lines. The analyzer grating, consisting of absorbing lines with the same periodicity and orientation as the fringes created by G_1 , is placed at a distance d , directly followed by the imaging detector system. In order to make a direct determination of the exact fringe position, micrometer spatial resolution in the detector plane would be needed, but for neutron imaging this is not available so far. Instead, the analyzer grating transforms the fringe positions into a measurable intensity modulation on the detector by a spatial phase stepping approach (Chant, 1995).

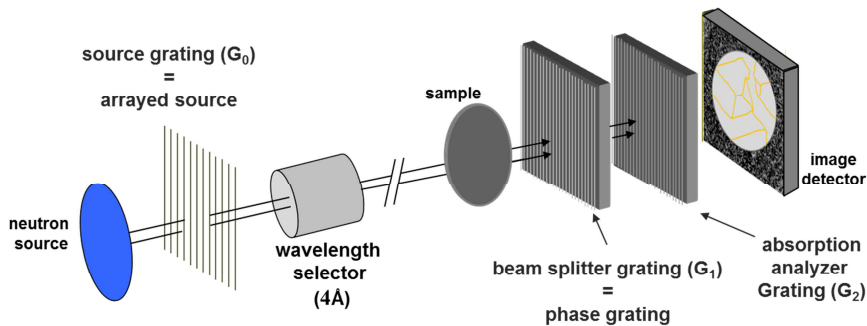


Fig. 1: schematic Setup with source, three gratings, wavelength selector, sample and detection system

1.2. Magnetic interaction

Like in optics, neutrons are refracted at surfaces where two different refractive indices meet. These different refractive indices may occur caused by different material properties (like the magnetic domain structure) or material compositions. Magnetic domain walls scatter incoming neutrons, because the complex refractive index of a material is depending on the magnetic induction B . In the case of a magnetic domain wall in a homogeneous material, the nuclear part of the refractive index does not change ($d_{\text{nuc}} = \text{const}$). The change of the refractive index (1) can, neglecting the attenuation, then be reduced to the magnetic contribution (d_{mag}) (2), which is given by (3), λ being the wavelength, μ_N the magnetic moment of the neutron, m the mass of the neutron and h the Planck constant.

$$n = 1 - \delta_{nuc} - \delta_{mag} + i\beta \quad (1)$$

$$\rightarrow n = 1 - \delta_{mag} \quad (2)$$

$$\rightarrow n = 1 \pm \frac{2\mu_N B m \lambda^2}{h^2} \quad (3)$$

Following equation (3) unpolarized neutrons are scattered at domain walls, where the magnetization changes. Calculated values for detectable scattering angles, for the setup parameters used at ICON, are in the range of: $\theta \approx 0.25$ mrad.

2. Grain-oriented steel laminations

2.1. Dark-field image of individually resolved domain walls

Grain oriented electrical steels provide very large grains and very large magnetic domains, with sizes up to mm in width and cm in length. In figure 2 a) a simple transmission image of a GO-sheet is shown. The sheet with a thickness of 300 μm is hardly visible, whereas in the DFI the sheet shows a clear contrast in b). On the one hand large horizontal black lines are visible on the other hand areas where the signal is degraded occur. The black lines represent 180°-domain walls, with the magnetization pointing from left to right or vice versa. The domains are oriented like this because of the very sharply textured material with the magnetic easy axis lying preferably in the rolling direction.

The darker areas with an averaged decreased signal are grains that are slightly misoriented. If a crystallographic grain is slightly misoriented, the stray field energy for large domains changes resulting in an energetically less favorable state. Small surface domains called supplementary lance leaf domains are generated. These supplementary domains are smaller than individually resolvable with the nGI, leading to an averaged signal decrease in the whole area, while the signal originating from the small surface domains superimposes the signal from a potentially underlying larger domain structure. The dark-field value is a measurable for the relative amount of domain walls and reduces the sensitivity for the investigation of individual domains in the specific pixel.

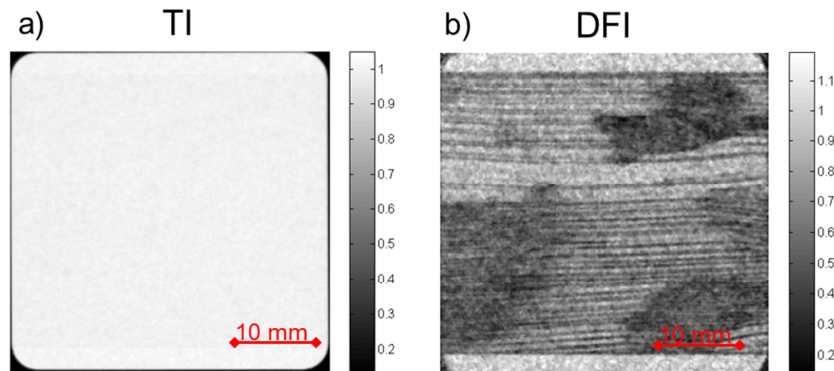


Fig. 2: a) Transmission image of a grain oriented electrical steel. The sheet (300 μm thickness) is hardly visible. b) The dark-field image reveals a strong contrast for the magnetic structure inside the sheet, showing domain walls of large, elongated magnetic domains but also areas with a decreased signal (misoriented grains).

The big advantage of the nGI-technique is that it reveals the magnetic structure in transmission. The information is an information about the whole volume. Even a dark-field tomography is possible if magnetic structural depth information is needed, although it is very time consuming. The tomographic reconstruction can be done by the use of filtered back-projection algorithm known from classical transmission tomography. It is so far the only technique

able to investigate a magnetic structure, spatially resolved, in a bulk sample nondestructively. The second advantage is the large field of view. Established magnetic imaging techniques like magneto-optical-Kerr-microscopy (MOKE) provide a field of view in the μm to mm range albeit they provide better spatial resolution.

3. Non-oriented steel laminations

3.1. Deterioration effects cause by production and cutting

In non-oriented steels a relative density distribution of domain walls is recorded instead of individually resolved domain walls due to the small size of the domains. These non-oriented sheets are widely used in industry as material for rotor and stator geometries in the field of electro mobility. During the production of the geometries the steel undergoes many different processing steps that influence the quality of the machine. One of these processing steps is the cutting of the steel for the final use. Different cutting techniques show different influences to the resulting performance of electrical devices. The magnetic behavior changes depending onto different cutting techniques that are investigated in figure 3.

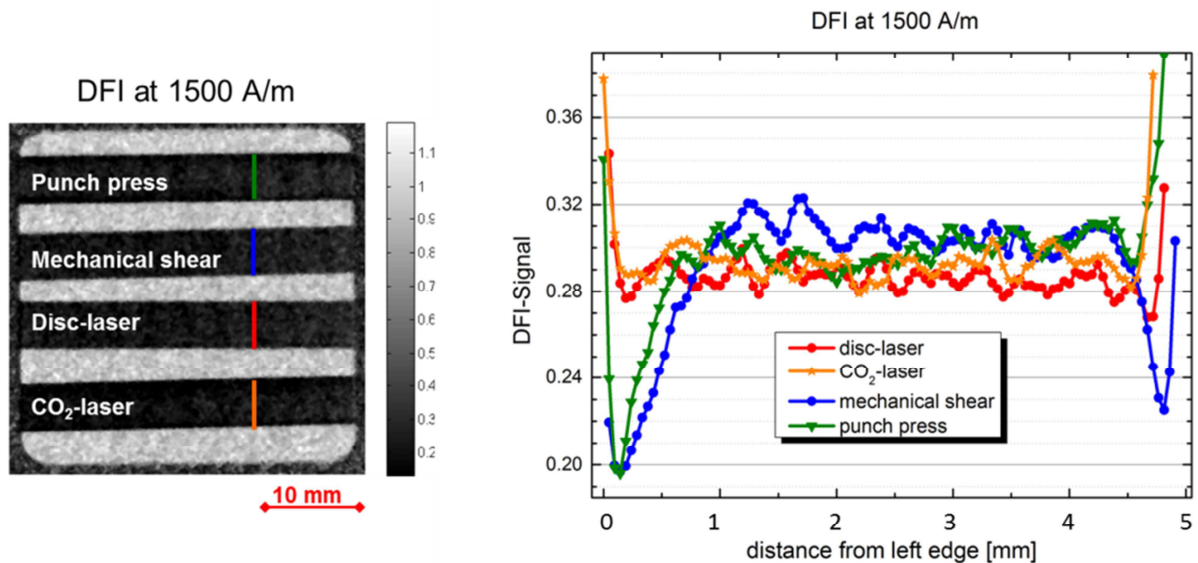


Fig. 3: DFI of four non-oriented electrical steel laminations produced by four different cutting processes. Two mechanical- and two laser-cut samples are shown. b) Plot along the coloured lines in the DFI. The bump of the signal near the edge for the mechanical cut samples is clearly noticeable, while the laser cut samples do not show an evident edge effect

The deterioration of the sheet near the cutting edge is visible in the DFI in 3 a). The deterioration leads to a higher amount of required energy to fully magnetize the steel in operation resulting in higher losses or less power of the electrical motor. With the help of the nGI technique these effects were investigated and characterized. The plot in figure 3 b) along the colored lines in the DFI (Fig. 3a)) shows the evident degradation of the signal in the area of the edge. The decrease of the signal is interpreted as a higher amount of domain walls. This higher amount leads to a worse magnetic behavior in respect to the magnetization of that device. It is known that mechanical cutting leads to microstructural changes like grain refinement or dislocation generation in the steel. Here the nGI enables an analysis for the influence of the cutting to the magnetic properties in a spatially resolved manner. The influence is about 2 μm deep inside the sample clearly recognizable. The punch pressed sample is only pressed on

one side and does only show a degradation of the signal at this side. The mechanical shear process shows the higher amount of domains on both sides.

The thermal methods (orange and red), where the cutting is realized by a laser, do not show an influence to the lamination at the edge, but a slightly reduced signal over the whole sample originating from thermal stresses introduced by the cutting.

References:

- P.H.Chant, P.J.Bryanston-Crosst, and S.C.Parker. Fringe-pattern analysis using a spatial phase-stepping method with automatic phase unwrapping. *Meas.Sci.Technol.* 6, 1250-1259 (1995)
- C. Grünzweig et al. Neutron Decoherence Imaging for Visualizing Bulk Magnetic Domain Structures. *Phys. Rev. Lett.* 101, 025504 (2008-I)
- C. Grünzweig et al. Bulk magnetic domain structures visualized by neutron dark-field imaging. *Appl. Phys. Lett.* 93, 112504(2008-II)
- C. Grünzweig, et al. Design, fabrication, and characterization of diffraction gratings for neutron phase-contrast imaging, *Rev. Sci. Instr.* 79, (2008-III)
- C. Grünzweig, et al. Multiple small angle neutron scattering: A new two dimensional ultra-small angle neutron scattering technique. *Appl. Phys. Lett.* 91, 203504 (2007)
- A.P. Kaestner, et al. The ICON beamline - A facility for cold neutron imaging at SINQ, *Nuc. Instr. Met.* 659, 387 (2011)
- F. Pfeiffer et al. Neutron phase imaging and tomography, *Phys. Rev. Lett.* 96, 215505, (2006)
- H.F.Talbot. Facts relating to optical science. *Phil. Mag* 9, 401-407 (1836)